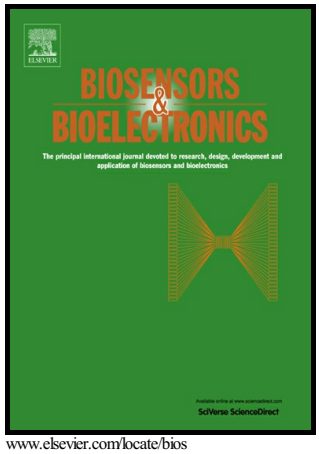

www.elsevier.com/locate/bios

A Non-Enzymatic Two Step Catalytic Reduction of Methylglyoxal by Nanostructured V_2O_5 Modified Electrode

Lakshmishri Ramachandra Bhat, Srinivasan Vedantham, Uma Maheswari Krishnan, John Bosco Balaguru Rayappan

PII: S0956-5663(17)30840-0
DOI: https://doi.org/10.1016/j.bios.2017.12.036
Reference: BIOS10181

To appear in: *Biosensors and Bioelectronic*

Received date: 11 October 2017
Revised date: 13 December 2017
Accepted date: 21 December 2017

Cite this article as: Lakshmishri Ramachandra Bhat, Srinivasan Vedantham, Uma Maheswari Krishnan and John Bosco Balaguru Rayappan, A Non-Enzymatic Two Step Catalytic Reduction of Methylglyoxal by Nanostructured V_2O_5 Modified Electrode, *Biosensors and Bioelectronic,* https://doi.org/10.1016/j.bios.2017.12.036

A Non-Enzymatic Two Step Catalytic Reduction of Methylglyoxal by Nanostructured V_2O_5 Modified Electrode

[1,2]Lakshmishri Ramachandra Bhat, [3,4]Srinivasan Vedantham, [1,3]Uma Maheswari Krishnan and [1,2]John Bosco Balaguru Rayappan

[1]Centre for Nanotechnology & Advanced Biomaterials (CeNTAB), SASTRA University, Thanjavur – 613 401, India

[2]School of Electrical & Electronics Engineering (SEEE), SASTRA University, Thanjavur – 613 401, India

[3]School of Chemical and Biotechnology (SCBT), SASTRA University, Thanjavur – 613 401, India

[4]Disease Program Lead-Diabetes, MedGenome Inc., Narayana Health City, Bangalore – 560 099, India

Corresponding author: *Prof. John Bosco Balaguru Rayappan School of Electrical & Electronics Engineering (SEEE) & Centre for Nanotechnology & Advanced Biomaterials (CeNTAB) SASTRA University, Thanjavur – 613 401, India Email: rjbosco@ece.sastra.edu

Tel.: +91 4362 264101-108 x2255; Fax: +91 4362 264120

Abstract

Methylglyoxal (MG) is a predominant precursor for advanced glycation end products (AGEs) due to its protein glycation reactions, which are the major causes of diabetic complications. MG is explored as a significant biomarker towards the prediction of diabetic complications. With this background, a non-enzymatic electrochemical biosensor has been developed to detect MG in human blood plasma samples. Microwave synthesized V_2O_5 nanoplates were used as interface material in the fabrication of modified gold (Au) working electrode for electrochemical MG biosensor. Orthorhombic crystal structured V_2O_5 with an oxidation state of +5 exhibited specific MG sensing performance. Cyclic voltammetry and amperometry studies confirmed the electrocatalytic nature of V_2O_5 nanoplates modified Au

electrode in the detection of MG. Non-enzymatic V_2O_5 modified Au electrode showed a sensitivity of 4.519 µA $µM^{-1}$ with a linear range of 3 to 30 µM, limit of detection (LOD) of 0.24 µM, limit of quantification (LOQ) of 0.80 µM and a response time less than 8 s towards MG. The lifetime and percentage recovery of the sensor was found to be 25 days (90%) and 102.5-108.7% respectively.

Graphical abstract

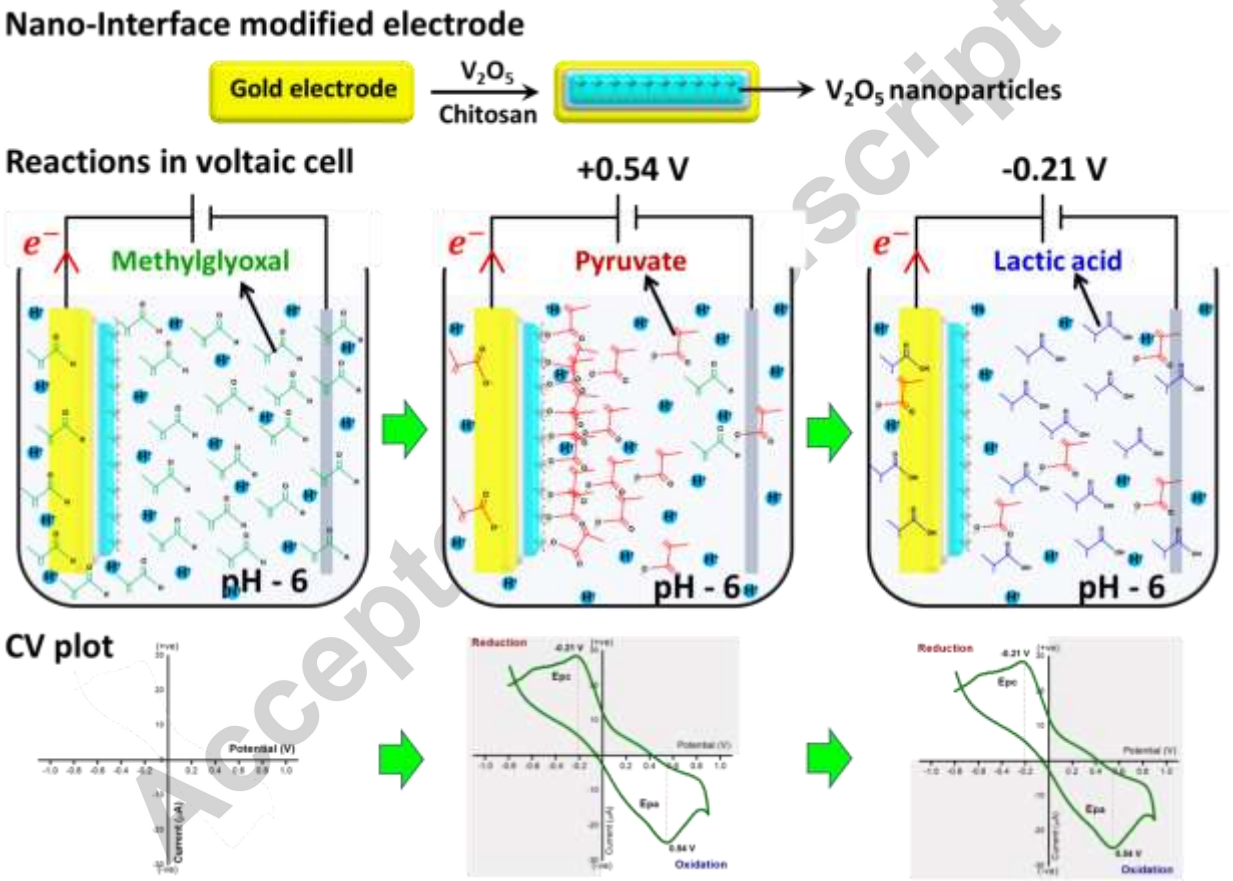

Keywords: Methylglyoxal; Electrochemical Biosensor; Vanadium pentoxide; Non-enzymatic detection; Blood Plasma.

1 Introduction

Diabetes mellitus (DM) is a devastating cause of several complications like cardiac and neurologic disorders (Ogawa et al., 2010) and a huge economic burden for countries all over the world (Dall et al., 2014). The seventh edition of International Diabetes Federation (IDF) Atlas reports more than 415 million diabetics, 193 million undiagnosed people and 318 million with impaired glucose tolerance (American Diabetes Association, 2014). Despite the steps taken by IDF and World Health Organization (WHO), the number of people with diabetes (Type 1, Type 2 and gestational diabetes) is increasing each year unrelentingly. DM (Baynes, 2015; Dall et al., 2014) is a chronic disorder characterized by the state of hyperglycemia for a prolonged duration, which gradually affects all the metabolic activities, especially, the vascular and neurological metabolism.

Glucose is the major sugar residue present in the body and hence many researchers have focused on enzymatic (Alwarappan, Liu, Kumar, & Li, 2010; Bharath et al., 2015; Sapountzi et al., 2017) and non- enzymatic glucose (Li et al., 2016; Madhu et al., 2015; Ngo, Hoa, Chung, & Hur, 2017; Wu et al., 2017) sensors development. Reduction of glucose with the reaction of amino groups in proteins results in Schiff bases and Amadori products and form intermediate products called as Advanced Glycation End products (AGEs). AGEs can be formed in all the stages of glycation process (Singh R , Barden A , Mori T, 2001; Thornalley, Langborg, & Minhas, 1999). The intermediate glycation reaction products known as oxoaldehydes are MG, glyoxal, 3-deoxyglucosone (3-DG), 4-hydroxynonenal and acrolein.

MG, 3-DG and glyoxal have formed from all stages of glycation reactions. In recent times, MG has drawn major attention, owing to its higher reactivity than glucose towards amino acids, (Mittelmaier & Pischetsrieder, 2011; Tauer et al., 2001; Wang, Lin, Spicer, & Stevens, 2015) cross-linking, role in the formation of irreversible AGEs and denaturation of proteins (Lo, Westwood, McLellan, Selwood, & Thornalley, 1994). Advanced glycation is a long-term reaction, and hence, the formation of MG is stable and independent of variation of glucose level in blood due to food habits. This function can be considered as a merit for the detection of MG for diabetes prediction than monitoring glucose level. In this scenario, development of electrochemical biosensors for the detection of MG has gained significant momentum due to the advantages of easy to handle, low-cost, rapid and portable (Chatterjee & Chen, 2012; Chatterjee, Wen, & Chen, 2013; Ezhilan et al., 2015; Thangavel et al., 2015) over the expensive and time-

consuming techniques like capillary electrophoresis (Zhang et al., 2010), colorimetric (Wang et al., 2015), high performance liquid chromatography (HPLC)(Kalapos, 1999), enzyme-linked immunosorbent assay (ELISA) (Inagi et al., 1999), and gas chromatography (Kalapos, 1999).

In the recent past, enzymatic (Alagappan et al., 2017; Ezhilan et al., 2015; Ramachandra, Vedantham, Krishnan, Nesakumar, & Balaguru Rayappan, 2016; Thangavel et al., 2015) and a few non-enzymatic (Chatterjee & Chen, 2012; Chatterjee et al., 2013) MG biosensors have been reported. Towards the specific detection of MG, glyoxalase-1 and glutathione enzymes were used in these sensors. The complicated handling procedures and short shelf life of enzyme activity in enzymatic sensors forced the scientific community to focus on non-enzymatic sensors. Chatterjee *et al.* have explored the electroactive surface of single wall carbon nanotubes (SWNT) (Chatterjee et al., 2013), and platinum nanoparticles on SWNT (Chatterjee & Chen, 2012) for the quantification of MG in human plasma and beer/wine samples respectively using square wave voltammetry technique.

In similar line, strong electrocatalytic and versatile redox properties of V_2O_5 nanostructures have been considered to favor the electron exchange in the chemical environment (Liu et al., 2015). Since, partially filled d-orbitals or valence states of vanadium atoms are extremely sensitive towards the chemical environment (Baddour-Hadjean et al., 2012), the same has been preferred as nanointerface for triggering redox reactions at the working electrode. The multi-valance states of vanadium ranging from V^{2+} to V^{5+}, chemical and thermal stability made V_2O_5 suitable for catalysis (Thiagarajan et al., 2016). It acts as an excellent catalyst for selective oxidation and reduction, dehydrogenation of hydrocarbons and other organic compounds (Thiagarajan et al., 2016).

In this work, non-enzymatic, mediator less MG sensor has been developed using V_2O_5 modified gold (Au) working electrode in buffer solution (pH 6) and human blood plasma. The sensor exhibited high sensitivity and swift response time. Moreover, conversion of MG to pyruvate and further to lactic acid by electrochemical means has been reported. The multi-valence states of V_2O_5 nanointerface along with the Au electrode were proved to be a promising combination for the reduction of MG. To the best of our knowledge, this is the first report on the V_2O_5/Au electrode as a non-enzymatic electrochemical sensor for the detection of MG in human blood plasma.

2 Experimental section

2.1 Materials and methods

MG, glyoxal, and acrolein were procured from Sigma-Aldrich (USA). Ammonium metavanadate was purchased from Nice - chemicals (India). Phosphate buffered saline (DPBS formula 10X) was purchased from Alfa Aesar (USA). All other chemicals such as sodium hydroxide (NaOH) pellets, glucose, chitosan, ascorbic acid, urea, 4-hydroxynonenal and acetic acid (degree of deacetylation of 82.5%, molecular weight 140,000g mol^{-1}) were purchased from Merck (India). All the reagents and solutions were prepared using double de-ionized water with electrical conductivity <1 μ℧ (Aqua purification system, India). Nickel chloride, zinc acetate dihydrate, and cupric acetate were obtained from Thermo Fisher Scientific (India). Cadmium acetate and uric acid were procured from Loba Chemie (India). Gold (Au) electrode (CHI 101, 2 mm diameter), Ag/AgCl reference electrode (CHI 111, 0.5 mm diameter) and platinum (Pt) counter electrode (CHI 115, 0.5 mm diameter) were purchased from CH Instruments (USA). V_2O_5 nanoplates were prepared using 0.05, 0.1 and 0.15 M concentration of ammonium metavanadate precursor *via* microwave synthesis method and labeled as V1, V2 and V3 respectively (Supplementary section 1.1).

2.2 Characterization techniques

Morphological and structural characteristics of V_2O_5 nanoplates were studied using Field Emission Scanning Electron Microscope (FE-SEM, JSM, 6701, JEOL, Japan) and X-ray Diffractometer (XRD, D8 Focus, Bruker, Germany) with Cu Kα radiation (1.5406 Å) respectively. X-Ray Photoelectron Spectrometer (XPS) (PHI Quantum 2000, Physical Electronics, Inc., USA) was used to analyze the chemical state of the elements in V_2O_5. Hall effect measurement system (HMS 3000, ECOPIA, S. Korea) was employed to measure the room temperature electrical properties of V_2O_5 like carrier concentration, and mobility using van der Pauw method.

Electrochemical studies were performed using the conventional three-electrode system employing electrochemical workstation (CH600C, CH Instruments, Inc., USA). Gold (Au) electrode as working (which was modified with V_2O_5 nanoplates at later stages), Ag/AgCl saturated with 0.4 M KCl as reference and Platinum (Pt) wire as counter electrodes were used for electrochemical experiments. Cyclic voltammetric and amperometric techniques were used for

electrochemical analysis of the bare and V_2O_5 nanoplates modified Au electrodes. 10X PBS was diluted to 1X (pH 7.3) and used as an electrolyte for the electrochemical experiments.

2.3 Fabrication of Au/ V_2O_5 Electrode

The Au working electrode was modified using the electrocatalytic V_2O_5 nanoplates (V1, V2 and V3). Prior to the modification, the electrode was cleaned using 1, 0.3 and 0.05 µ sized alumina powders and washed with distilled water to obtain mirror shine surface. Further, the electrode was ultrasonicated for 2 min before immobilizing the matrix. The Au electrode was chosen to satisfy the need of wide range of scanning potential and low susceptibility to oxide formation and surface contamination. Also, Au electrode favors the reduction of MG to pyruvate (Chadderdon et al., 2015). Further immobilizing matrix was prepared using chitosan and V_2O_5 samples. The biodegradable polymer chitosan acts as a carrier agent of MG and other therapeutic molecules for anticancer treatment (Chakrabarti, Talukdar, Pal, & Ray, 2014). Thus, strong tendency of attracting or binding MG of chitosan molecule motivated to be used as a binder. 2 mg of V_2O_5 sample was dispersed in a solution containing 40 µL of chitosan (0.1 wt./v% of deacetylated chitosan using 2% acetic acid in 10 mL deionized water) and 100 µL of deionized water. This mixture was further ultrasonicated for 20 min and mixed well in vortex machine for 2 min. 3 µL of this well dispersed solution was drop casted on to the Au electrode and dried at room temperature.

3 Results and discussion

3.1 Structural and morphological studies

Fig. 1 (a) shows the XRD patterns of V1, V2 and V3 nanoplates. All the observed patterns can be indexed to the orthorhombic crystal structure of α- V_2O_5 belonging to the P*mmn* space group 59 (JCPDS #89-0612). The major peaks at 2θ angles of 20.2, 26.0, and 30.9 were assigned to the (001), (110), and (301) planes respectively. The growth of (001) plane due to the influence of molar concentration confirmed the formation of the two-dimensional layered structure of edge- and corner-sharing, square VO_5 pyramids (Filonenko, Sundberg, Werner, & Zibrov, 2004). On the other hand, α- V_2O_5 also exhibited a three-dimensional network of edge- and corner-sharing VO_6 octahedra, which is parallel to (001) plane (Filonenko et al., 2004). Sizes of the oriented crystalline domains along the planes (001), (110), and (301) were calculated using Scherrer's formula $d = k\lambda/\beta \cos\theta$, where λ is the wavelength of X-ray radiation (1.5406 Å), β

is the full width half maximum of the corresponding plane, θ is the Bragg angle, and k is the shape factor (0.9) and are presented in Table S1 (Supplementary Section). The crystallite size of (001) plane increased from 26 to 39 nm with an increase in the molar concentration from 0.05 to 0.15 M. Shoulder formation in the XRD patterns for 0.05, 0.10 and 0.15 M precursor concentrations revealed the presence of pores existing in the samples (Eren & Afsin, 2008). It clearly exhibited the growth of two-dimensional layered structure with (001) plane orientation tends to the development of larger crystallites, which has also been confirmed by the FESEM images.

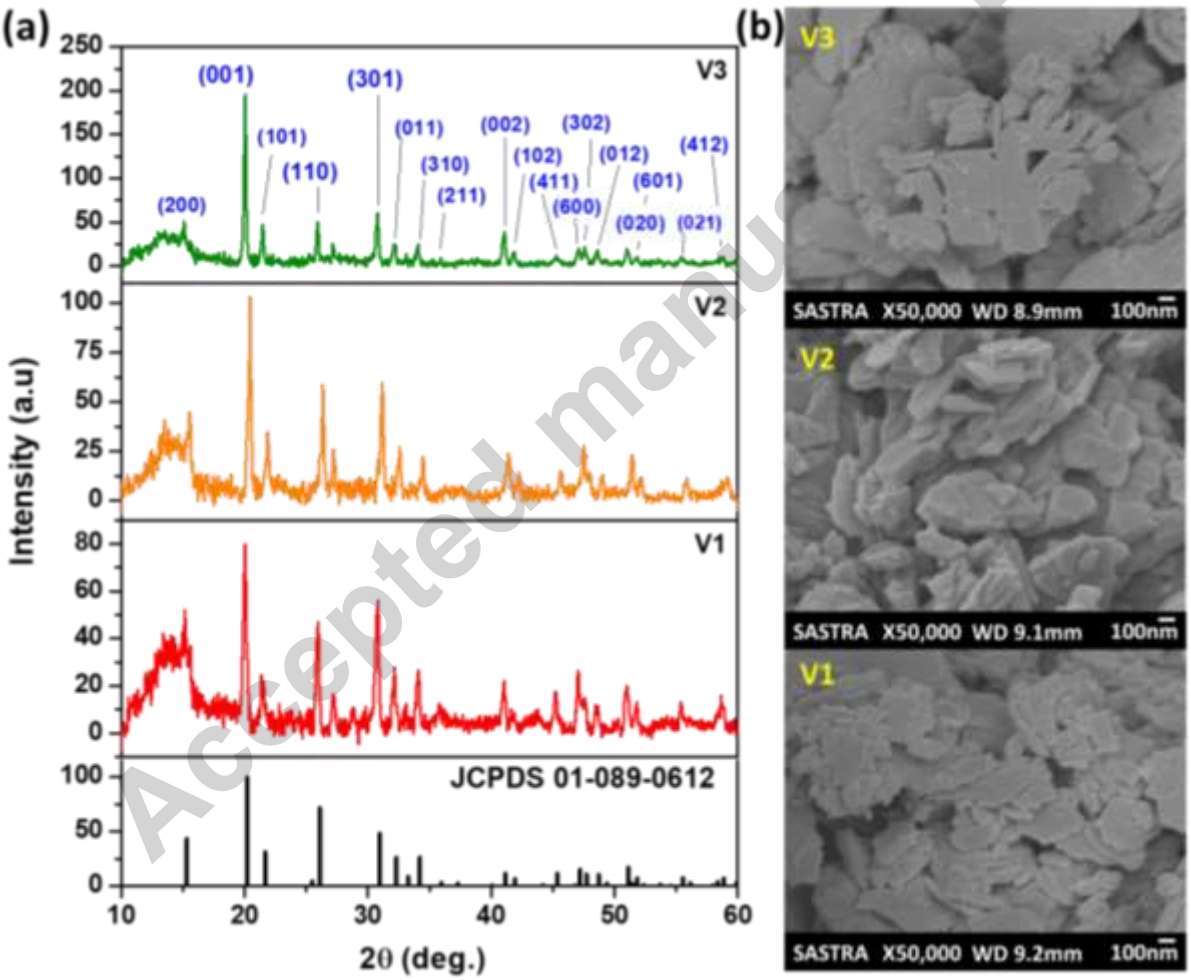

Fig. 1. (a) XRD patterns and **(b)** FE-SEM images of V_2O_5 samples V1, V2, and V3.

FE-SEM images (Fig. 1 (b)) show the formation of irregular bunches of nanoplates (V1), individually defined nanoplates (V2) and agglomerated small units of nanoplates (V3) for the precursor concentrations of 0.05, 0.10 and 0.15 M respectively. Similar kind of morphology was obtained while preparing V_2O_5 nanostructures using commercially available V_2O_5 nanoparticles

through autoclave method (C. Zhang et al., 2016). Also, the observed nanoplates and layered sheet kind of morphology might be due to the characteristics of two-dimensional layered orthorhombic V_2O_5 (Kumar, Qadir, Maury, & Bahlawane, 2017) as confirmed by the XRD pattern with (001) as a dominant plane. FESEM images also confirmed the formation of Edge-, corner-sharing, square VO_5 pyramids, which were observed in the XRD patterns. Further, the porous nature of nanoplates indicated by the shoulder formation in the XRD pattern can be seen in the FESEM images.

3.2 Composition and electronic structure analysis

Fig. 2 shows the narrow survey spectra of V_2O_5 samples from 510 to 535 eV. The observed XPS signals have undergone a Gaussian curve fitting process to detect the oxygen and different vanadium cation oxidation states. The core-level spectra of V 2p spin-orbit split into $2p_{3/2}$ and $2p_{1/2}$ doublet followed by O 1s were observed. The binding energy of 517.68 and 524.77 eV for core-level V 2p doublet (difference of 7 to 8 eV) and 530 eV for O 1s were observed by the standard energy pattern of V_2O_5 (Silversmit, Depla, Poelman, Marin, & De Gryse, 2004; Yin, Yu, Song, Huang, & Zhu, 2014). The oxidation states of vanadium (V^{5+}, V^{4+} and V^{3+}) represent the formation of V_2O_5, VO_2, and V_2O_3 compounds respectively. The corresponding binding energies of the core-level V $2p_{3/2}$ of V^{5+}, V^{4+}, V^{3+}, V^{2+}, and V^{0+} were 517.2, 515.84, 515.29, 513.67, and 512.35 eV respectively (Silversmit et al., 2004). In all the three samples, V 2p spectra exhibited a strong mainline peak at 517.2±0.5 eV, which confirmed the V^{5+} oxidation state and formation of V_2O_5. The full width at half maximum (FWHM) of V $2p_{3/2}$ peak is 3.54, 2.44, and 2.79 eV towards V1, V2 and V3 respectively. The reduction in the FWHM represents the formation of highly oxidized V_2O_5 surface (Mendialdua, Casanova, & Barbaux, 1995). The high vanadium concentration induced variation in the surface density of vanadium in V3 sample favored the highly oxidized V_2O_5 surface in-turn eliminated the formation of other compounds. The observed high donor carrier concentration (Fig. S1, Supplementary section 1.2) for V3 sample was confirmed by the narrow peak of V $2p_{3/2}$ from XPS spectra. The O 1s spectra showed the formation of overlapped components. The main peak at 529.2±0.2 eV signal assigned to the chemical state of oxygen bonded with vanadium (Mendialdua et al., 1995). The second component at 531.33, 530.56 and 530.42 eV were observed for V1, V2, and V3 samples respectively (Zimmermann, Claessen, Reinert, Steiner, & Hüfner, 1999). The second component

shifted towards lower binding energy for V3 and the improved crystallinity of V3 sample observed from XRD spectra supported the same.

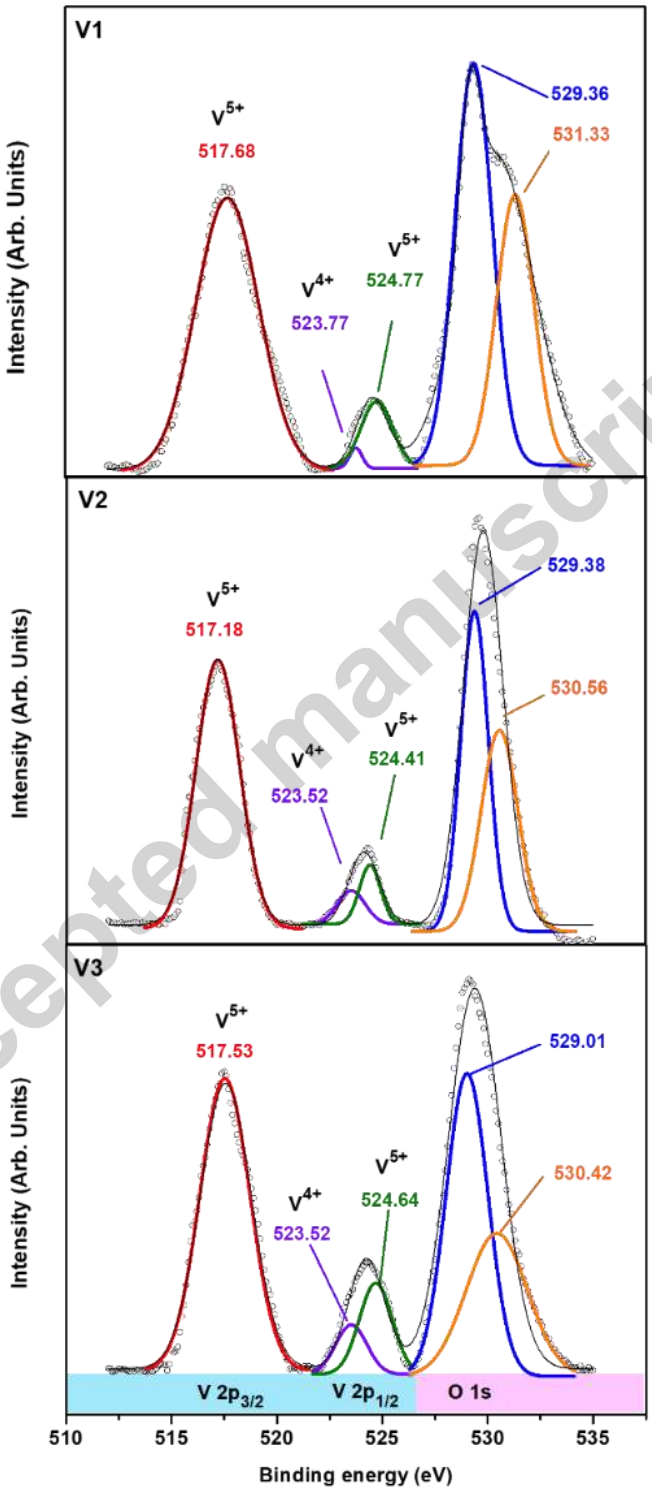

Fig. 2. XPS narrow survey spectra of core-level V 2p and O 1s of the prepared V_2O_5 samples.

3.3 Electrochemical studies

3.3.1 Characterization of modified electrodes

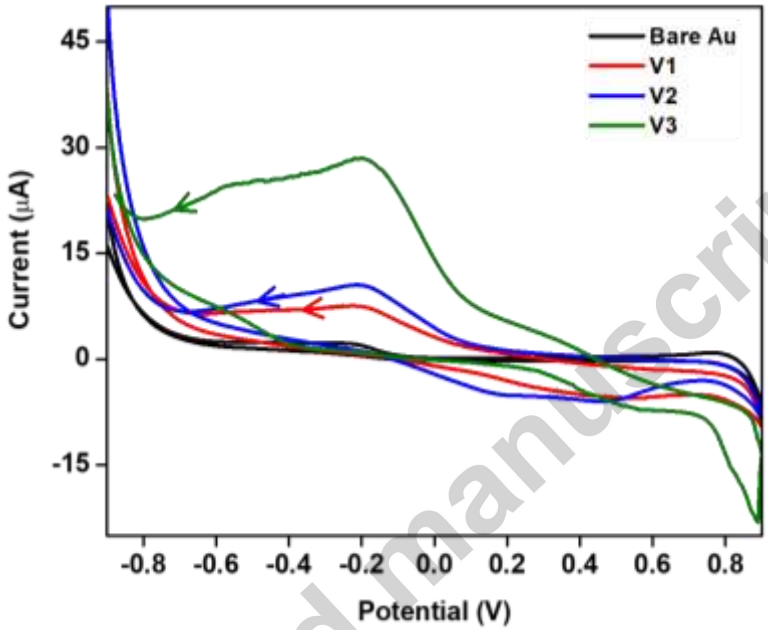

Fig. 3. Cyclic voltammograms recorded for modified electrodes in the presence of 100 µM MG in 1X PBS at a scan rate of 0.01 Vs^{-1}.

Fig. 3 shows the cyclic voltammogram obtained for the Au and modified Au electrodes in the presence of MG. To analyze the performance of V_2O_5 nanointerface in detecting MG, the bare Au and other modified electrodes were subjected to cyclic voltammetric studies in the presence of 100 µM of MG at the scan rate of 0.01 Vs^{-1} in 1X PBS of pH 7.4. The absence of redox peaks in the presence and absence of MG showed that bare Au electrode was not responding to MG. Whereas, Au modified electrodes showed peaks at 0.54 and -0.21 V in the presence of MG, which revealed the electron transfer process initiated by catalytic V1, V2, V3 interfaces. Both the peaks were in good accordance with the reported literature for the formation of pyruvate ions and subsequently lactic acid (Fig. 3) (Chadderdon et al., 2015; Lim, Tan, & Turpin, 2013; Yang et al., 2015). The overall reaction mechanism is discussed in section 3.4.7.

Table 1. Electrochemical parameters of various modified electrodes.

Modified electrodes	E (V)		E° (V)	ΔE (V)	I (μA)		K_S (s^{-1})		Q (x 10^{-4} C)	Γ (x 10^{-8} M cm^{-2})
	Anode	Cathode			Anode	Cathode	Anode	Cathode		
V1	-0.224	0.441	0.108	0.665	5.383	7.931	0.008	0.012	6.427	1.060
V2	-0.217	0.453	0.118	0.67	5.951	10.588	0.006	0.010	9.880	1.630
V3	-0.210	0.547	0.169	0.755	6.976	28.233	0.011	0.046	6.066	1.00

3.3.2 Comparison of electrochemical parameters

The electrochemical parameters obtained for each modified electrode were compared to analyze their performance (Table 1). The peak potentials, peak currents, electron transfer constants obtained for cathodic and anodic processes, charge consumed, and surface coverage of each electrode were compared (Supplementary section 1.3). Among the three modified electrodes, electrode modified with V3 sample showed better results interms of peak potential and current, electron transfer rate, and charge consumption. Hence, V3 modified electrode was chosen as the best among the three modified electrodes and used for further experiments.

Optimization of scan rate, pH, and incubation time were carried out to obtain maximum performance of the V3 modified electrode toward MG detection. Scan rate was fixed as 0.08 Vs^{-1}, pH was optimized as 6 and incubation time was set as 5 min for further experiments (Supplementary section 1.4).

3.3.3 Sensing mechanism

The possible reaction mechanism of MG into lactic acid in the presence of nanointerface *via* intermediate reaction pathways of pyruvate ions is shown in Fig. 4 (Chadderdon et al., 2015; Lim et al., 2013; Yang et al., 2015).

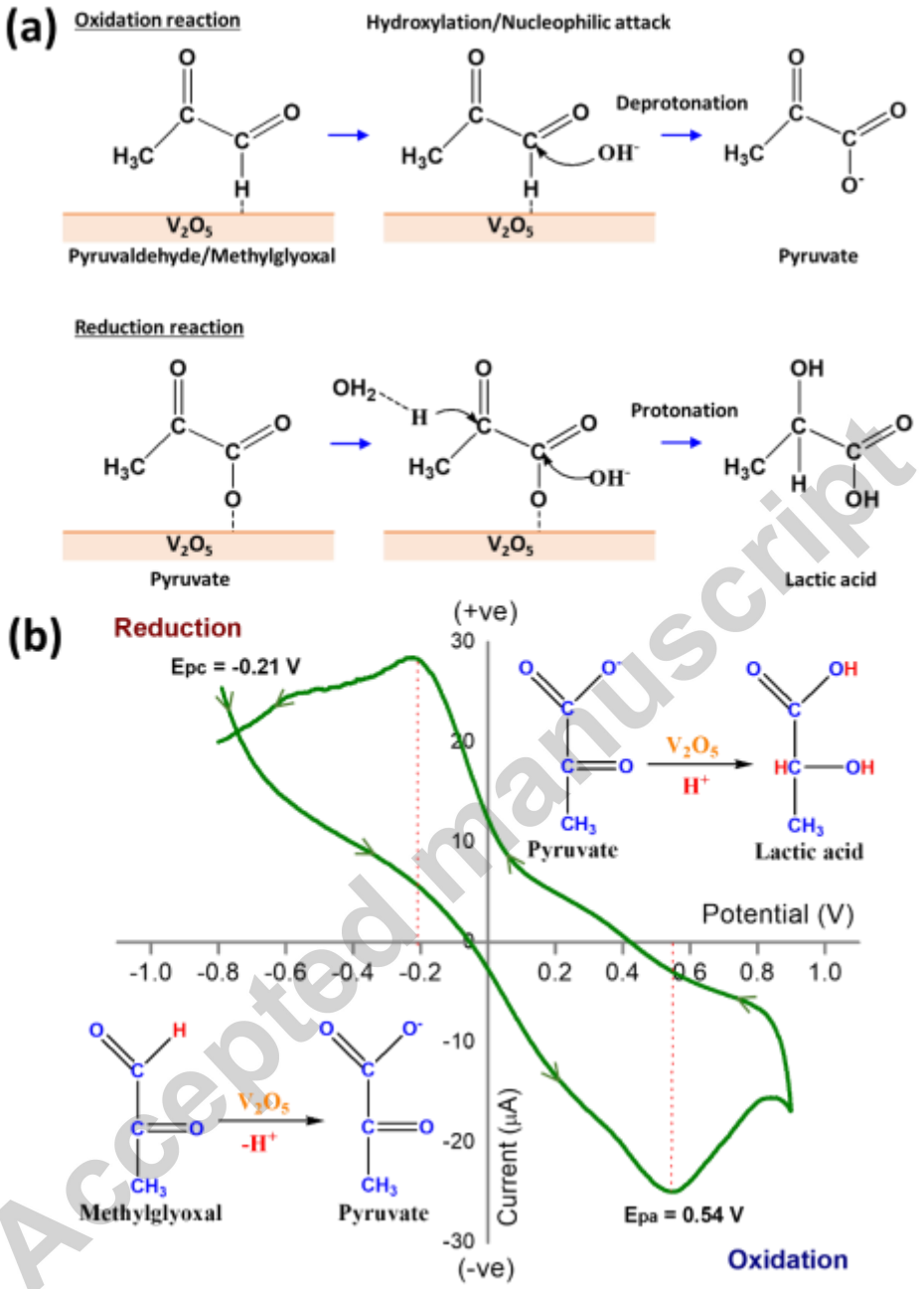

Fig. 4 (a) Reduction reaction of MG in the electrochemical cell and **(b)** mechanism of MG sensing andcorresponding electrochemical reactions occurring in the electrochemical cell.

The reaction mechanism depicted in Fig. 4 describes the reduction of pyruvaldehyde (MG) to pyruvate and further to lactic acid. The reduction of pyruvaldehyde to pyruvate occured *via* hydroxylation followed by deprotonation and nucleophilic attack on its carbonyl group. Initially, when the applied potential was negative, electrons from cathode moved to the solution resulting in the decreased anodic current. During the positive potential sweep, pyruvaldehyde

molecules bound to the V_2O_5 nanointerface and undergone deprotonation at the aldehyde group and resulted in the formation of pyruvate ions at 0.54 V (Fig. 4b). Subsequently, in the second sweep, pyruvate ions experienced reduction at the carbonyl group and formed the lactic acid at the negative potential of -0.210 V (Fig. 4b). The interaction of hydronium and hydroxyl ions on pyruvate ions led to the formation of lactic acid due to the electrocatalytic property of V_2O_5 (Fig. 4a). In other case, pyruvaldehyde (MG) could have directly reduced to lactic acid through intramolecular Cannizzaro reaction (Chadderdon et al., 2015; Lim et al., 2013; Yang et al., 2015) with hydride shift and protonation by the Lewis acids (V^{4+} ions). In the current work, the reaction scheme has not occurred as a single step but happened in two steps; deprotonation of MG forming pyruvate at 0.54 V and subsequently conversion into lactic acid at -0.210 V (Fasman, 1989). The electron shuttling property of V_2O_5 interface on Au electrode might have catalyzed the production of pyruvate and sequential deprotonation and protonation of species existing in the solution.

3.3.4 Effect of MG concentration

Fig. 5 (a) shows the cyclic voltammetry curves obtained for V3 modified electrode towards 5 to 95 µM concentration of MG in the electrochemical cell containing 5 mL of 1X PBS. The observed cathodic peak current exponentially decreased with an increase in MG concentration having correlation coefficient R^2 of 0.97 (Fig. 5 (b)). An exponential decrease of current with increasing analyte concentration might be due to the saturation of V_2O_5 active sites or protonation process. The electrochemical conversion of pyruvaldehyde to lactic acid *via* intermediate reaction of pyruvate ions depend on the protonation process (Scheme 1). Also, ionic conditions (pH = 6) have to be favorable for the reduction process (Fig. S3(a)). The reduction process of oxidized pyruvate ions to lactic acid exhibited maximum electron transfer between nanointerface and electrolyte. At lower concentrations, reduction process was strong enough as the availability of hydrogen ions was high. As the analyte concentration increased, the reduction rate of pyruvate ions decreased. It can be explained by the simple electron-transfer reaction and proton-coupled electron-transfer reactions (Savéant, 2007; Zhao, Lu, Bond, & Zhang, 2012). The higher concentration of pyruvate ions occupied the nanointerface surface get reduced by protonation process. Due to the lack of hydrogen ions (pH = 6) required for the protonation process of pyruvate ions, the reaction rate decreased exponentially with an increase in MG

concentration. Similar kind of decrease in exponential peak current concerning analyte concentration was reported (Kuznetsov, Shumakovich, Koroleva, & Yaropolov, 2001) due to charge accumulation.

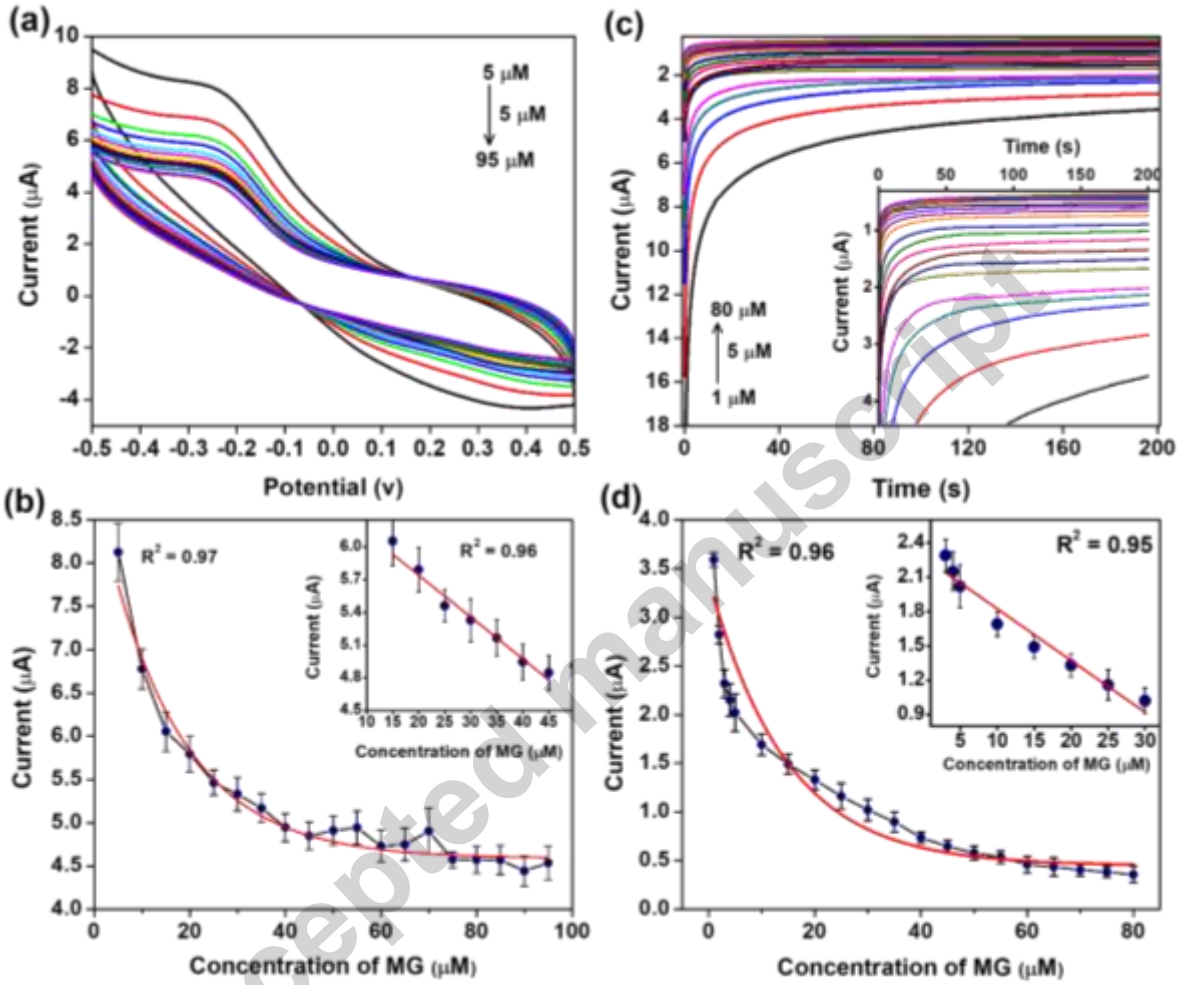

Fig. 5 (a) Cyclic voltammogram plot and **(b)** measured current response from CV plot, **(c)** amperometric study and **(d)** measured current response from the amperometric plot of V3 nanoplates modified Au electrode at scan rate 0.08 Vs^{-1} in 1X PBS of pH 6 for various concentration of MG.

The exhibited maximum current response at lower concentrations can be considered as an advantage when deployed in real-time sample analysis. Inset in Fig. 5 (b) shows the calibration curve for the concentration 15 – 45 μM of MG. The linear regression equation obtained for modified electrode is $I = -3.835\ \mu A\ [S] + 6.509$ with a correlation coefficient $R^2$of 0.96, where

I is the current response and S is the MG concentration. The lowest MG concentration detected (limit of detection LOD) in cyclic voltammetry was 0.33 µM and the limit of quantification was found to be 1.09 µM.

The amperometric study was carried out to obtain the specific response of Au/V3 electrode for MG at -0.210 V (Fig. 5(c)). The amperometric responses towards 1 to 80 µM concentrations of MG in steps of 5 µM for 200 s each were observed. The same trend of decrease in current response as observed in CV has been confirmed. This has again confirmed the requirement of hydrogen ions for the protonation of pyruvate ions to form lactic acid. The current response was linear over a range of 3 to 30 µM with R^2 of 0.95 (Fig. 5(d)). The sensitivity of the developed sensor was found to be 4.519 µA μM^{-1}. The current response was decreased linearly with LOD of 0.24 µM, LOQ of 0.80 µM and the response time was <8 s.

3.3.5 Repeatability and reproducibility

The repeatability and reproducibility of the V3 modified electrode were determined by repeating the fabrication of the modified electrode using drop casting procedure for 5 times. The observed inter- and intra-assay precisions signified that the procedure used for the fabrication of V3 modified electrode was standardized and the same was verified with a very low RSD value of 1.03% and 1.00% respectively. It also showed that immobilization of V_2O_5 and chitosan was crack free and stable on the Au electrode.

3.3.6 Interferents study

To confirm the selectivity of the V3 modified electrode, it was subjected to potential interferents, which can inhibit the detection of MG in real time samples. Hence, glyoxal, acrolein, and 4-hydroxynonenal, which are known as dicarbonyl compounds having very similar chemical structure and bonding as MG were considered for this study. 100 µL from 0.1 mM of other dicarbonyl compounds were added to the PBS containing 40 µM MG. The modified electrode showed no characteristic current response in the presence of other dicarbonyl compounds. The observed selectivity might be due to the potential dependence of V_2O_5 nanointerface, which might have catalytically influenced only MG. Apart from these dicarbonyl compounds, influence of common interfering species like ascorbic acid, glucose, urea, uric acid

and metal ions like Zn^{2+}, Ni^{2+}, Cu^{2+}, and Cd^{2+} was also investigated. There were negligible variations in the current response when the interferents were introduced in to the electrolyte.

The %Inhibition (Table S2) was calculated using the following formula:

$$\%Inhibition = \frac{I_o - I_i}{I_o} \quad (5)$$

where, I_o and I_i represent the current response (in µA) in the absence and presence of inhibitor respectively. The very low values of %Inhibition showed that V3 modified electrode was very much selective towards MG and capable of overcoming all the considered potential interferents.

3.3.7 Life time

Stability of V3 modified electrode was confirmed by checking its current response in the presence of 5 µM of MG regularly once per day for 25 days. The dry stability of the electrode at room temperature was observed to be 90% after 25 days.

3.3.8 Determination of MG in human blood plasma

Recovery studies were performed to check the applicability of the developed electrode in detecting MG in real time samples. 5 mL of human blood was collected and centrifuged at 8000 rpm for 15 min to separate the blood cells and plasma. The collected supernatant sample was used for the analysis of MG by diluting 30 µL in 30 mL of PBS. The 100 µL of diluted sample was added to the electrochemical cell containing 5 mL of PBS. Known concentrations of MG were spiked in to the electrochemical cell, and their corresponding current responses were recorded. %Recovery (Table S3) was calculated as a measurement of the accurate prediction of the analyte level in real time samples using the formula given below:

$$\text{Recovery (\%)} = \frac{MG\ detected}{MG\ added} \times 100 \quad (6)$$

Recovery% (Table S3) in the range of 102.5-108.7% with an RSD ranging from 1.47-3.53% was obtained for the developed V3 modified electrode, which confirmed its applicability of its usage in detecting MG in real time samples. It also implied that the electrode is capable of

detecting the target MG molecules in the presence of potential interferents. Table S4 shows the comparison of this work with the existing MG sensors.

4 Conclusion

An enzyme free electrochemical sensor using V_2O_5 nanointerface was developed and standardized for the detection of MG. Experimental parameters like pH, scan rate, and incubation time were standardized to obtain specific sensing response towards MG. The developed MG sensor exhibited figure of merits like LOD of 0.24 µM, LOQ of 0.80 µM with a response time of <8 s and a linear range from 3 - 30 µM. Agglomerated small units of V_2O_5 nanoplates with high crystallinity and carrier concentration aided in enhancing electron transfer rate between MG and Au electrode with a maximum rate constant. V^{4+} ions of V_2O_5 nanointerface acted as the site of initiation of decomposition of MG in two intermediate steps resulting in the formation of pyruvate ions and lactic acid respectively. High current response for lower concentrations of MG proved as an advantage for the sensor to be deployed in real time scenario, where very low concentration of MG can be detected with higher response. MG sensor showed a life time of 25 days and a recovery% ranging from 102.5-108.7% in human blood plasma samples.

Conflict of interest

The authors declare no conflict of interest.

Acknowledgements

One of the authors Lakshmishri Ramachandra Bhat sincerely thanks the Council of Scientific and Industrial Research for fellowship under Senior Research Fellowship Scheme (09/1095/0012/2016-EMR-I). Authors extend their thanks to Nano Mission Council (No.SR/NM/PG–16/2007), Department of Science & Technology, India (SR/FST/ETI-284/2011(C)) for the financial support. We also acknowledge SASTRA University for the infrastructural support.

References

Alagappan, L. P., Shanmugasundaram, P., Ramachandra, B. L., Gumpu, M. B., Nesakumar, N., Jayanth Babu, K., … Balaguru Rayappan, J. B. (2017). Fabrication of electrochemical biosensor with vanadium pentoxide nano-interface for the detection of methylglyoxal in rice. *Analytical Biochemistry*, *528*, 19–25. https://doi.org/10.1016/j.ab.2017.04.010

Alwarappan, S., Liu, C., Kumar, A., & Li, C. Z. (2010). Enzyme-doped graphene nanosheets for enhanced glucose biosensing. *Journal of Physical Chemistry C*, *114*(30), 12920–12924. https://doi.org/10.1021/jp103273z

American Diabetes Association. (2014). National Diabetes Statistics Report , 2014 Estimates of Diabetes and Its Burden in the Epidemiologic estimation methods. *National Diabetes Statistics Report*, 2009–2012.

Baddour-Hadjean, R., Smirnov, M. B., Smirnov, K. S., Kazimirov, V. Y., Gallardo-Amores, J. M., Amador, U., … Pereira-Ramos, J. P. (2012). Lattice Dynamics of β-V_2O_5: Raman Spectroscopic Insight into the Atomistic Structure of a High-Pressure Vanadium Pentoxide Polymorph. *Inorganic Chemistry*, *51*(5), 3194–3201. https://doi.org/10.1021/ic202651b

Baynes, H. W. (2015). Classification, Pathophysiology, Diagnosis and Management of Diabetes Mellitus. *Journal of Diabetes & Metabolism*, *6*(541), 1–9. https://doi.org/10.4172/2155-6156.1000541

Bharath, G., Madhu, R., Chen, S.-M., Veeramani, V., Balamurugan, A., Mangalaraj, D., … Ponpandian, N. (2015). Enzymatic electrochemical glucose biosensors by mesoporous 1D hydroxyapatite-on-2D reduced graphene oxide. *J. Mater. Chem. B*, *3*(7), 1360–1370. https://doi.org/10.1039/C4TB01651C

Chadderdon, D. J., Xin, L., Qi, J., Brady, B., Miller, J. A., Sun, K., … Li, W. (2015). Selective Oxidation of 1,2-Propanediol in Alkaline Anion-Exchange Membrane Electrocatalytic Flow Reactors: Experimental and DFT Investigations. *ACS Catalysis*, *5*(11), 6926–6936. https://doi.org/10.1021/acscatal.5b01085

Chakrabarti, A., Talukdar, D., Pal, A., & Ray, M. (2014). Immunomodulation of macrophages by methylglyoxal conjugated with chitosan nanoparticles against Sarcoma-180 tumor in mice. *Cellular Immunology*, *287*(1), 27–35. https://doi.org/10.1016/j.cellimm.2013.11.006

Chatterjee, S., & Chen, A. (2012). Voltammetric detection of the dicarbonyl compound: Methylglyoxal as a flavoring agent in wine and beer. *Analytica Chimica Acta*, *751*, 66–70. https://doi.org/10.1016/j.aca.2012.09.011

Chatterjee, S., Wen, J., & Chen, A. (2013). Electrochemical determination of methylglyoxal as a

biomarker in human plasma. *Biosensors and Bioelectronics*, *42*(1), 349–354. https://doi.org/10.1016/j.bios.2012.10.091

Dall, T. M., Yang, W., Halder, P., Pang, B., Massoudi, M., Wintfeld, N., … Hogan, P. F. (2014). The economic burden of elevated blood glucose levels in 2012: Diagnosed and undiagnosed diabetes, gestational diabetes mellitus, and prediabetes. *Diabetes Care*, *37*, 3172–3179. https://doi.org/10.2337/dc14-1036

Eren, E., & Afsin, B. (2008). An investigation of Cu (II) adsorption by raw and acid-activated bentonite : A combined potentiometric , thermodynamic , XRD , IR , DTA study, *151*, 682–691. https://doi.org/10.1016/j.jhazmat.2007.06.040

Ezhilan, M., Alagesan, S., Ramachandra, B. L., Gumpu, M. B., Nesakumar, N., Vedantham, S., … Rayappan, J. B. B. (2015). Chemometric Analysis for the Determination of Methylglyoxal in Grilled Chicken Using ZnO Flakes Based Glyoxalase 1 Biosensor. *Sensor Letters*, *13*(3), 245–253. https://doi.org/10.1166/sl.2015.3425

Fasman, G. D. (Ed.). (1989). Physical and chemical data. In *Practical handbook of biochemistry and molecular biology* (pp. 122–130). CRC Press.

Filonenko, V. P., Sundberg, M., Werner, P.-E., & Zibrov, I. P. (2004). Structure of a high-pressure phase of vanadium pentoxide, β-V2O5. *Acta Crystallographica Section B Structural Science*. https://doi.org/10.1107/S0108768104012881

Inagi, R., Miyata, T., Yamamoto, T., Suzuki, D., Urakami, K., Saito, A., … Kurokawa, K. (1999). Glucose degradation product methylglyoxal enhances the production of vascular endothelial growth factor in peritoneal cells: role in the functional and morphological alterations of peritoneal membranes in peritoneal dialysis. *FEBS Letters*, *463*(3), 260–264. https://doi.org/10.1016/S0014-5793(99)01642-7

Kalapos, M. P. (1999). Methylglyoxal in living organisms - Chemistry, biochemistry, toxicology and biological implications. *Toxicology Letters*, *110*(3), 145–175. https://doi.org/10.1016/S0378-4274(99)00160-5

Kumar, S., Qadir, A., Maury, F., & Bahlawane, N. (2017). Visible thermochromism in vanadium pentoxide coatings. *ACS Applied Materials & Interfaces*.

https://doi.org/10.1021/acsami.7b04484

Kuznetsov, B. A., Shumakovich, G. P., Koroleva, O. V., & Yaropolov, A. I. (2001). On applicability of laccase as label in the mediated and mediatorless electroimmunoassay: Effect of distance on the direct electron transfer between laccase and electrode. *Biosensors and Bioelectronics*, *16*(1–2), 73–84. https://doi.org/10.1016/S0956-5663(00)00135-4

Li, S.-J., Hou, L.-L., Yuan, B.-Q., Chang, M.-Z., Ma, Y., & Du, J.-M. (2016). Enzyme-free glucose sensor using a glassy carbon electrode modified with reduced graphene oxide decorated with mixed copper and cobalt oxides. *Microchimica Acta*, *183*(6), 1813–1821. https://doi.org/10.1007/s00604-016-1817-4

Lim, Y. B., Tan, Y., & Turpin, B. J. (2013). Chemical insights, explicit chemistry, and yields of secondary organic aerosol from OH radical oxidation of methylglyoxal and glyoxal in the aqueous phase. *Atmospheric Chemistry and Physics*, *13*(17), 8651–8667. https://doi.org/10.5194/acp-13-8651-2013

Liu, B., Li, X., Zhao, Q., Liu, J., Liu, S., Wang, S., & Tadé, M. (2015). Insight into the mechanism of photocatalytic degradation of gaseous o-dichlorobenzene over flower-type V2O5 hollow spheres. *J. Mater. Chem. A*, *3*(29), 15163–15170. https://doi.org/10.1039/C5TA02295A

Lo, T. W. C., Westwood, M. E., McLellan, A. C., Selwood, T., & Thornalley, P. J. (1994). Binding and Modification of Proteins by Methylglyoxal under Physiological Conditions. *The Journal of Biological Chemistry*, *269*(51), 32299–32305.

Madhu, R., Veeramani, V., Chen, S. M., Manikandan, A., Lo, A. Y., & Chueh, Y. L. (2015). Honeycomb-like Porous Carbon-Cobalt Oxide Nanocomposite for High-Performance Enzymeless Glucose Sensor and Supercapacitor Applications. *ACS Applied Materials and Interfaces*, *7*(29), 15812–15820. https://doi.org/10.1021/acsami.5b04132

Mendialdua, J., Casanova, R., & Barbaux, Y. (1995). XPS studies of V_2O_5, V_6O_{13}, VO_2 and V_2O_3. *Journal of Electron Spectroscopy and Related Phenomena*, *71*(3), 249–261. https://doi.org/10.1016/0368-2048(94)02291-7

Mittelmaier, S., & Pischetsrieder, M. (2011). Multistep Ultrahigh Performance Liquid

Chromatography/Tandem Mass Spectrometry Analysis for Untargeted Quantification of Glycating Activity and Identification of Most Relevant Glycation Products. *Analytical Chemistry*, *83*, 9660–9668.

Ngo, Y.-L. T., Hoa, L. T., Chung, J. S., & Hur, S. H. (2017). Multi-dimensional Ag/NiO/reduced graphene oxide nanostructures for a highly sensitive non-enzymatic glucose sensor. *Journal of Alloys and Compounds*, *712*, 742–751. https://doi.org/10.1016/j.jallcom.2017.04.131

Ogawa, S., Nakayama, K., Nakayama, M., Mori, T., Matsushima, M., Okamura, M., … Ito, S. (2010). Methylglyoxal is a predictor in type 2 diabetic patients of intima-media thickening and elevation of blood pressure. *Hypertension*, *56*(3), 471–476. https://doi.org/10.1161/HYPERTENSIONAHA.110.156786

Ramachandra, B. L., Vedantham, S., Krishnan, U. M., Nesakumar, N., & Balaguru Rayappan, J. B. (2016). Estimation of methylglyoxal in cow milk – an accurate electrochemical response time based approach. *Anal. Methods*, *8*(10), 2207–2217. https://doi.org/10.1039/C5AY02901E

Sapountzi, E., Braiek, M., Vocanson, F., Chateaux, J. F., Jaffrezic-Renault, N., & Lagarde, F. (2017). Gold nanoparticles assembly on electrospun poly(vinyl alcohol)/poly(ethyleneimine)/glucose oxidase nanofibers for ultrasensitive electrochemical glucose biosensing. *Sensors and Actuators, B: Chemical*, *238*, 392–401. https://doi.org/10.1016/j.snb.2016.07.062

Savéant, J. M. (2007). Electrochemical concerted proton and electron transfers. Further insights in the reduction mechanism of superoxide ion in the presence of water and other weak acids. *Journal of Physical Chemistry C*, *111*(7), 2819–2822. https://doi.org/10.1021/jp068322y

Silversmit, G., Depla, D., Poelman, H., Marin, G. B., & De Gryse, R. (2004). Determination of the V2p XPS binding energies for different vanadium oxidation states (V5+ to V0+). *Journal of Electron Spectroscopy and Related Phenomena*, *135*(2–3), 167–175. https://doi.org/10.1016/j.elspec.2004.03.004

Singh R , Barden A , Mori T, B. L. . (2001). Advanced glycation end-products: a review . *Diabetologia*, *44*(2), 129–146.

Tauer, A., Knerr, T., Niwa, T., Schaub, T. P., Lage, C., Passlick-Deetjen, J., & Pischetsrieder, M. (2001). In vitro formation of N-epsilon-(carboxymethyl)lysine and imidazolones under conditions similar to continuous ambulatory peritoneal dialysis. *Biochemical and Biophysical Research Communications*, *280*(5), 1408–1414. https://doi.org/10.1006/bbrc.2001.4294

Thangavel, A., Alagesan, S., Nesakumar, N., Ramachandra, B. L., Gumpu, M. B., Vedantham, S., … Rayappan, J. B. B. (2015). Optimization of Electrochemical Parameters for Specific Blood Methylglyoxal Determination Using ZnO Sepals Based Glyoxalase 1 Biosensor. *Sensor Letters*, *13*(4), 328–337. https://doi.org/10.1166/sl.2015.3439

Thiagarajan, S., Thaiyan, M., Ganesan, R., Wu, Y., Xu, P., & Liu, J. (2016). Physical vapor deposited highly oriented V_2O_5 thin films for electrocatalytic oxidation of hydrazine. *RSC Advances*, *6*(86), 82581–82590. https://doi.org/10.1039/C6RA09109A

Thornalley, P. J., Langborg, A., & Minhas, H. S. (1999). Formation of glyoxal, methylglyoxal and 3-deoxyglucosone in the glycation of proteins by glucose. *Biochemical Journal*, *344*(1), 109–116. https://doi.org/10.1042/bj3440109

Wang, S.-T., Lin, Y., Spicer, C. D., & Stevens, M. M. (2015). Bio-inspired Maillard-Like reactions enable a simple and sensitive assay for colorimetric detection of methylglyoxal. *Chemical Communications*, *51*(55), 11026–11029. https://doi.org/10.1039/C5CC02590G

Wu, K.-L., Cai, Y.-M., Jiang, B.-B., Cheong, W.-C., Wei, X.-W., Wang, W., & Yu, N. (2017). Cu@Ni core–shell nanoparticles/reduced graphene oxide nanocomposites for nonenzymatic glucose sensor. *RSC Adv.*, *7*(34), 21128–21135. https://doi.org/10.1039/C7RA00910K

Yang, L., Su, J., Carl, S., Lynam, J. G., Yang, X., & Lin, H. (2015). Catalytic conversion of hemicellulosic biomass to lactic acid in pH neutral aqueous phase media. *Applied Catalysis B: Environmental*, *162*(August 2014), 149–157. https://doi.org/10.1016/j.apcatb.2014.06.025

Yin, H., Yu, K., Song, C., Huang, R., & Zhu, Z. (2014). Synthesis of Au-Decorated V2O5@ZnO Heteronanostructures and Enhanced Plasmonic Photocatalytic Activity. *ACS Applied Materials & Interfaces*, *6*, 140827145709006. https://doi.org/10.1021/am501549n

Zhang, C., Fang, G., Liang, C., Zhou, J., Tan, X., Pan, A., & Liang, S. (2016). Template-free synthesis of highly porous V_2O_5 cuboids with enhanced performance for lithium ion batteries. *Nanotechnology*, *27*(30), 305404. https://doi.org/10.1088/0957-4484/27/30/305404

Zhang, J., Zhang, H., Li, M., Zhang, D., Chu, Q., & Ye, J. (2010). A novel capillary electrophoretic method for determining methylglyoxal and glyoxal in urine and water samples. *Journal of Chromatography A*, *1217*(31), 5124–5129. https://doi.org/10.1016/j.chroma.2010.05.040

Zhao, S. F., Lu, J. X., Bond, A. M., & Zhang, J. (2012). Remarkable sensitivity of the electrochemical reduction of benzophenone to proton availability in ionic liquids. *Chemistry - A European Journal*, *18*(17), 5290–5301. https://doi.org/10.1002/chem.201103365

Zimmermann, R., Claessen, R., Reinert, F., Steiner, P., & Hüfner, S. (1999). Strong hybridization in vanadium oxides: evidence from photoemission and absorption spectroscopy. *Journal of Physics: Condensed Matter*, *10*(25), 5697–5716. https://doi.org/10.1088/0953-8984/10/25/018

Highlights

- Non-enzymatic methylglyoxal (MG) sensor developed using V_2O_5 nanointerface
- Orthorhombic layered V_2O_5 nanoplates were synthesized using microwave technique
- Electrochemical reduction of MG to lactic acid *via* intermediate pyruvate ions was observed
- MG sensor exhibited sensitivity of 4.519 µA μM^{-1} with a linear range from 3 to 30 µM
- Developed sensor was used for the determination of unknown concentration of MG in human blood plasma samples with a recovery of 102.5-108.7%